ABDOMINAL IMAGING

ORIGINAL ARTICLE

Comparison of spin-echo echo-planar imaging magnetic resonance elastography with gradient-recalled echo magnetic resonance elastography and their correlation with transient elastography

Jin Woo Yoon
Eun Sun Lee
Hyun Jeong Park
Sung Bin Park
Young Youn Cho
Stephan Kannengiesser
Joonho Hur

PURPOSE

This study aimed to assess the agreement between liver stiffness (LS) values obtained by the gradient-recalled echo (GRE) magnetic resonance elastography (MRE) and spin-echo echo-planar imaging (SE-EPI) MRE with those of transient elastography (TE), respectively.

METHODS

We retrospectively included 48 participants who underwent liver MRE with both GRE and SE-EPI sequences in the same session and also TE within 1 year. We obtained LS values for MRE by drawing free-hand region of interest, and TE was performed using a FibroScan device. We assessed the relationship between the mean LS values obtained by each MRE sequence and TE using the correlation coefficients and Bland–Altman plots, respectively. We also compared LS values and technical failure rates of measured values from MRE between SE-EPI and GRE sequences using the paired t-test and McNemar's test. The MRE failure was defined as the absence of pixel value with a confidence index above 95%.

RESULTS

The LS values from SE-EPI and GRE sequences strongly correlated with those from TE (GRE; $r = 0.73$, $P < .001$ vs. SE-EPI; $r = 0.79$, $P < .001$). In addition, the LS values from the 2 MRE sequences showed excellent relationship (intraclass correlation coefficient, 0.94 [0.89-0.97], $P < .001$). The LS values from SE-EPI and GRE MRE were not significantly different (4.14 kPa vs. 3.88 kPa, $P = .19$). Furthermore, the technical success rate of SE-EPI MRE was superior to that of GRE (100% vs. 83.8%, $P = .031$).

CONCLUSION

The measured LS values obtained using TE correlated strongly with those obtained using GRE and SE-EPI MRE techniques, even though SE-EPI-MRE resulted a higher technical success rate than GRE-MRE. Therefore, we believe that TE, GRE, and SE-EPI MR elastography techniques may complement each other according to the appropriate individual situation.

From the Department of Radiology (J.W.Y., E.S.L. ✉ seraph377@cau.ac.kr, H.J.P., S.B.P., J.H.), and Department of Internal Medicine (Y.Y.C.), Chung-Ang University Hospital, Chung-Ang University College of Medicine, Heukseok-ro, Dongjak-gu, Republic of Korea; Siemens Healthcare GmbH (S.K.), Erlangen, Germany.

Currently, hepatic fibrosis is considered to have the potential to be reversed with treatment, especially during the early stages, but can progress to cirrhosis if left untreated.[1-3] Thus, the identification and staging of fibrosis prior to the development of liver cirrhosis (LC) are important when managing chronic liver disease (CLD),[4] which includes chronic hepatitis, alcoholic liver disease, and non-alcoholic fatty liver disease (NAFLD).

Variable non-invasive techniques for evaluating liver fibrosis including transient elastography (TE), ultrasound shear wave elastography, and magnetic resonance elastography (MRE) have been developed.[5-7] Among these techniques, TE, which measures the velocity of acoustic shear waves traveling the liver using ultrasound,[8] is the most validated and highly reproducible technique for diagnosing liver fibrosis.[9-11] However, high failure rates and unreliable measurements in patients with obesity or ascites are known to be major weaknesses of TE.[12,13]

Meanwhile, MRE is the non-invasive imaging modality available with the highest diagnostic accuracy in evaluating liver elasticity.[14-16] Based on magnetic resonance imaging (MRI), the

propagating shear waves through the liver are imaged and processed using an algorithm to generate cross-sectional images displaying the magnitude of the complex shear modulus.[17] Compared to ultrasound-based techniques, MRE can provide more comprehensive liver imaging examinations and larger coverage.[17,18]

Until recently, the most common pulse sequence used for MRE has been based on gradient-recalled echo (GRE) sequence, after being well-validated for liver stiffness (LS) evaluation by many previous studies.[17,19,20] However, GRE MRE is known to be more sensitive to T2* decay, which results in a high technical failure rate in the iron-overloaded liver.[20] On the other hand, the spin-echo echo-planar imaging (SE-EPI) MRE sequence, a relative newcomer, is less affected by transverse relaxation signal decay[21,22] and has resulted in a higher overall technical success rate than GRE MRE with shorter acquisition time and no significant difference in LS values.[17,20,23]

In the context of developing the appropriate clinical approach for non-invasive assessment of liver fibrosis, there is intense interest in the correlation between alternative techniques. In several studies comparing TE and GRE MRE, MRE has been found to be generally superior to TE in diagnosing hepatic fibrosis.[16,24,25] However, there are only a few studies comparing SE-EPI MRE and TE,[26] and there is no published study so far as we know that compares the LS values obtained by GRE MRE, SE-EPI MRE, and TE in the same study participants.

Accordingly, the purpose of this study is to assess the agreement between the LS values obtained by GRE MRE and SE-EPI MRE with those obtained by TE, respectively. In addition, we aimed to compare the LS values and technical success rates obtained by GRE MRE and SE-EPI MRE in the same setting.

Main points

- The liver stiffness (LS) values measured by transient elastography (TE) and those of gradient-recalled echo (GRE) and spin-echo echo-planar imaging (SE-EPI) MRE techniques are strongly correlated with one another.

- The technical success rate of SE-EPI MRE was superior to that of GRE MRE without a significant difference in LS values.

- Therefore, TE, GRE, and SE-EPI MRE techniques may complement each other in appropriate individual situations.

Methods

Patients

This study was approved by our institutional review board (approval no.: 2001-002-19296), and the requirement for informed consent was waived due to the retrospective nature of this study. Between April 2018 and December 2019, we identified 476 MREs, which were performed using both GRE and SE-EPI techniques, as part of the routine liver MR examination at our hospital. Of these, 49 patients had undergone TE within a 1-year interval. Of these 49 patients, we excluded patients with too many or too large hepatic masses to draw a region of interest (ROI) in the liver parenchyma, but only one patient was excluded because of a large hepatic mass (n = 1). None of the studies had technical errors to exclude in our study. Finally, 48 patients (mean age, 61 years; range, 30-80 years) were included in our study. The indications for liver MR examination included hepatocellular carcinoma (HCC) screening or surveillance (n = 40; 83.3%), other hepatic malignancy such as metastases (n = 5; 10.4%), benign focal hepatic lesions (n = 2; 4.2%), and others (n = 1; 2.1%).

MRI and MRE acquisition

All patients were scanned using a 3T MR unit (MAGNETOM Skyra; Siemens Healthcare) equipped with a 30-element body array coil and an integrated 32-element spine array coil. The patients were instructed to fast for 4-6 hours before the scan to reduce potential confounding factors. The MR sequences for the routine liver protocol consisted of the following sequences: breath-hold axial and coronal T2-weighted half-Fourier acquisition single-shot fast spin-echo, axial T1-weighted dual-echo (in-phase and opposed-phase), breath-hold T2-weighted fast spin-echo with fat suppression, axial diffusion-weighted imaging, and axial 3D fat-suppressed T1-weighted imaging before and after the intravenous contrast injection.

Liver MRE series were obtained before the intravenous administration of contrast agent (gadoxetic acid, Primovist®). The MRE wave was generated with a passive acoustic driver placed against the anterior body wall over the right hemi-liver. Continuous vibrations at 60 Hz were generated by the active acoustic driver (Resondant) through a tube to the passive driver, to induce shear wave propagation in the liver. For the GRE sequence, 4 axial sections through the liver were acquired in 4 consecutive end-expiratory breath-holds with a total acquisition time of 76 s. For the SE-EPI MRE sequence, all 4 sections were obtained in a single end-expiratory 11-second breath-hold. The detailed parameters of the MRE scan are shown in Table 1. The images depicting the relative tissue shear stiffness (elastogram) in kilopascals (kPa) were created by automatically processing the wave images by the MR scanner in measurable gray scale and a color overlay. In addition, to exclude regions of less reliable data, the process provided superimposed "confidence" maps with a checkerboard pattern overlaid on the elastograms with corresponding confidence values of less than 95%.

Analysis of MRE

All MRE data were analyzed by 2 radiologists (an abdominal radiologist with 10 years of experience and a second-year resident in training) in consensus to establish appropriate ROI for each data set. Two reviewers performed LS measurements by drawing free-hand ROIs on the grayscale elastogram of liver, avoiding large vessels, liver margins, and space-occupying lesions. A total of 8 ROI values could be obtained if all sequences were successful in both GRE and SE-EPI sequences. The reliable areas for measurement, without a checkerboard pattern, in each image slices were also obtained. Technical failure of MRE was determined if the area of pixel value with a confidence index above 95% and/or imaged apparent shear waves were absent.[20] The overall mean LS values of each patient were obtained by calculating the average of each ROI, weighted by ROI size, according to RSNA QIBA profile. The median ROI areas in 4 sections in each MRE sequence were calculated, if possible.

Failure factors of MRE

Clinical and radiologic data were reviewed to collect clinical factors that might be related to the technical failure of an MRE, including body mass index (BMI), the presence of ascites, iron deposition, a morphological feature of the liver (cirrhosis vs. non-cirrhosis), and the etiology of liver disease. We also assessed the Child–Turcotte–Pugh (CTP) score in cases with cirrhotic liver. The presence and amount of ascites were assessed using a 4-degree scale as follows: 0, none; 1, small; 2, moderate; and 3,

Table 1. Imaging parameters of GRE versus SE-EPI MRE

Parameter	GRE MRE	SE-EPI MRE
Pulse sequence type	GRE	EPI
Matrix	128 × 76	100 × 100
Field of view (cm)	380 × 226	380 × 380
TR/TE (ms)	50/23.75	1000/47
Bandwidth (Hz/pixel)	260	2380
No. of sections	4	4
Section thickness (mm)	5	6
Flip angle (degree)	25	90
Gap (mm)	10	12
MEG frequency (Hz)	60	60
Motion encoding direction	z	z
No. of breath holds	4	1
Acquisition time (s)	76 (19 × 4 sections)	11

GRE, gradient-recalled echo; SE-EPI, spin-echo echo-planar imaging; MRE, magnetic resonance elastography; TE, echo time; TR, repetition time; MEG, motion encoding gradient.

Table 2. Characteristics of the study population

Patient characteristics Total (n = 48)	Age (years), mean (range)	61 (30-80)
	Sex (male/female)	28/48 (58%)/20/48 (42%)
Indications for MRE	HCC screening/surveillance	40/48 (83.3%)
	Other malignant lesions	5/48 (10.4%)
	Benign focal liver lesions	2/48 (4.2%)
	Others	1/48 (2.1%)
BMI(kg/m^2), mean (range)		24.1 (18.8-30.5)
<30		45/48 (93.7%)
>30		3/48 (6.3%)
LC, 38/48 (79%)	CTP A	32/38 (84.2%)
	B	5/38 (13.1%)
	C	1/38 (2.6%)
Non-LC, 10/48 (21%)	CLD	8/10 (80%)
	Normal liver	2/10 (20%)
Ascites	None	34/48 (70.8%)
	Small	12/48 (25%)
	Moderate	1/48 (2.1%)
	Massive	1/48 (2.1%)
Etiologies of liver disease	HBV	26/48 (54.2%)
	HCV	3/48 (6.3%)
	Alcohol abuse	10/48 (20.8%)
	Autoimmune	1/48 (2.1%)
	NAFLD	1/48 (2.1%)
	Other	7/48 (14.6%)
Iron deposition		1/48 (2.1%)

MRE, magnetic resonance elastography; HCC, hepatocellular carcinoma; BMI, body mass index; LC, liver cirrhosis; CTP, Child–Turcotte–Pugh; CLD, chronic liver disease; HBV, hepatitis B virus; HCV, hepatitis C virus; NAFLD, non-alcoholic fatty liver disease.

massive amount of ascites. Significant iron accumulation was evaluated with the automatically calculated R2* (1/T2*) value from a 3-dimensional (3D) multi-echo Dixon sequence[27] (LiverLab; Siemens Healthcare). A significantly increased iron accumulation was defined as an R2* value of greater than or equal to 115 per second.[28] The cirrhotic morphology of liver was determined based on other routine liver MRI sequences such as T2-weighted imaging.

Transient elastography

All patients underwent TE using a FibroScan device by experienced sonographers, according to the previously described methods.[8] The patients were asked to fast for at least 4 h before the examination and were scanned by applying a 3.5 MHz ultrasound transducer (M-probe) mounted on a vibrator. The vibrator generated shear stress of 50 Hz (amplitude, 2 mm), and the induced shear wave propagated through the liver, which is also tracked using the co-axial ultrasound transducer. At least 10 TE measurements were performed for each patient to obtain valid LS values in kPa, and a median value was obtained. Reliable measurements were defined as: (i) a median value of 10 valid measurements[24] and (ii) an interquartile range (IQR=difference between the 75th and 25th percentiles of the data) divided by the median LS measurement value ≤30%.[29]

Statistical analysis

The results are presented as mean or median values (and 95% CIs) for quantitative data. The relationships between the mean LS values obtained by each MRE sequence and TE were analyzed using correlation coefficients. The Bland–Altman plots were generated separately for pooled data to assess agreement between both MRE and TE-derived LS values. We used the TE to MRE ratios instead of the differences for the Bland–Altman plots because the variability of the differences increases as the magnitude of the LS measurement increases. The patients were categorized into chronic hepatitis B (CHB) group and non-CHB group based on etiology of liver disease. The correlation coefficients values according to etiology (CHB group vs. non-CHB group) and liver morphology (cirrhosis vs. non-cirrhosis) were compared using Fisher Z test. The mean LS values and the median areas of confidence for LS measurement between SE-EPI and GRE MRE in the same participants were compared using
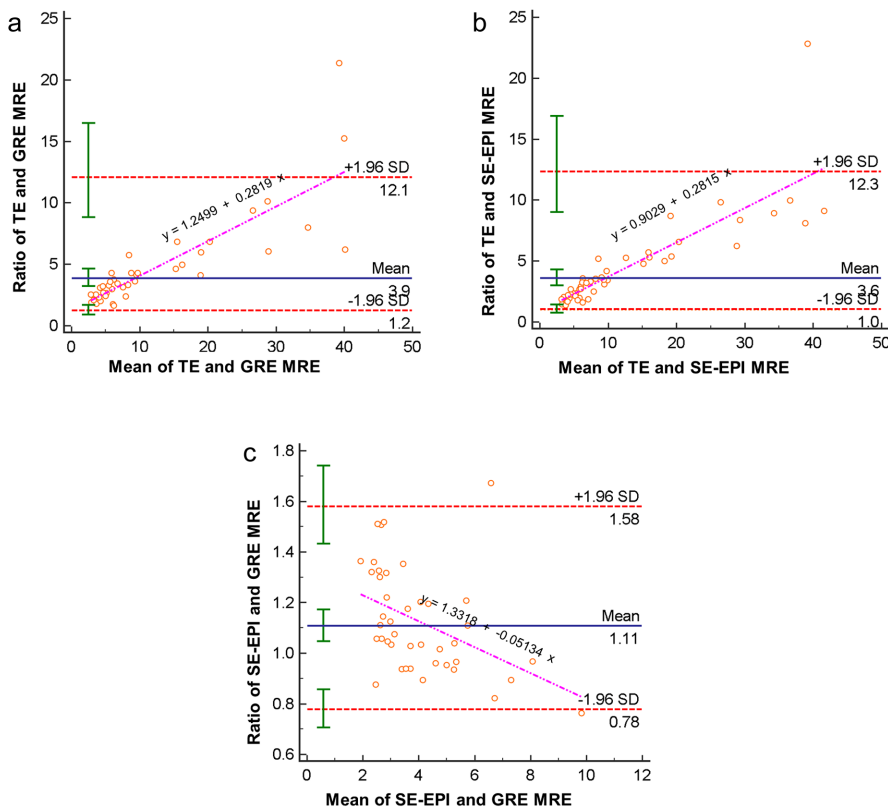
Figure 1. a-c. Bland–Altman plots (a-c) are generated with data from mean liver stiffness values based on GRE and SE-EPI MRE sequences and TE; the dotted red lines indicate 1.96 standard deviations above and below the mean and the solid green whiskers indicate the 95% prediction limits of the standard deviations and the pink line indicates the regression line. MRE, magnetic resonance elastography; GRE, gradient recalled echo; SE-EPI, spin-echo echo-planar imaging; TE, transient elastography; SD, standard deviation.

the paired t-test. Furthermore, McNemar's test was used to compare the technical success rates of MRE in SE-EPI and GRE. To identify factors associated with MRE failure, univariable logistic regression analyses were performed. MedCalc® software (version 19.1) was used for the statistical analysis and a 2-sided P value of less than .05 was considered statistically significant.

Results

We assessed a total of 48 pairs of MRE and TE examinations in this study. There were no technical issues preventing the acquisition of either sequence. The median time interval between MRE and TE was 29 days (range, 0-338 days). The mean BMI was 24.1 ± 2.8 kg/m² (range, 18.8-30.5 kg/m²).

Of the 48 patients, the majority (n = 38) had LC, 8 showed CLD configuration, and normal liver configuration was seen in 2 patients. Regarding the ascites, 46 patients had no or scanty amount of ascites, whereas the other 2 patients manifested with moderate or massive amount of ascites. The etiologies of liver disease were as follows: CHB (n = 26; 54.2%), chronic hepatitis C (CHC) (n = 3; 6.3%), alcohol abuse (n = 10; 20.8%), autoimmune hepatitis

(n = 1; 2.1%), NAFLD (n = 1; 2.1%), and others (n = 7; 14.6%). Only one of the patients showed significantly increased iron deposition; R2* value: 187.5/s (n = 1; 2.1%). The detailed patient characteristics are presented in Table 2.

The average of LS values measured with TE was 21.1 kPa (range, 3.8-75.0 kPa). The LS values from GRE and SE-EPI MRE strongly correlated with those from TE (GRE $r = 0.73$, $P < .001$ vs. SE-EPI $r = 0.79$ [0.66-0.88], $P < .001$). In addition, agreement was excellent between the measured LS values at the 2 MRE sequences (intraclass correlation coefficient, 0.94 [0.89-0.97], $P < .001$). Bland–Altman analysis demonstrated mean ratios of 3.86 (TE/GRE range, 1.24-12.06, $P < .001$) and 3.58 (TE/SE-EPI range, 1.04-12.32, $P < .001$) between the LS values from TE and each MRE sequences, respectively. It also showed that TE to MRE ratio tends to increase as the mean of TE LS and MRE LS increases. A total of 47 out of 48 patients' LS values (97.9%) and 40 out of 42 patients' LS values (95.2%) fell within the 95% prediction limits of agreement for SE-EPI MRE versus TE and GRE MRE versus TE, respectively (Figure 1).

Correlation between LS from SE-EPI MRE and TE was significantly weaker in the CHB group than in the non-CHB group (CHB $r = 0.50$ [0.14-0.74] vs. non-CHB $r = 0.93$ [0.84-0.97], $P < .001$). Conversely, a correlation between LS from GRE MRE and TE in the CHB and non-CHB groups was not statistically significant (CHB $r = 0.58$ [0.22-0.80] vs. non-CHB $r = 0.80$ [0.55-0.92], $P = .16$) (Table 3).

When the etiology was adjusted, the correlation between LS from MRE and TE was significantly stronger in the non-LC group than in the LC group in both MRE sequences; the results were as follows: non-LC versus LC group, SE-EPI_TE ($r = 0.96$ vs. 0.78, $P = .003$), GRE_TE ($r = 0.96$ vs. 0.70, $P = .001$) (Table 3).

The LS values for the individual patients as measured ranged from 1.62 to 11.14 kPa (median, 3.40 kPa) at GRE MRE and from 2.20 to 8.50 kPa (median, 3.81 kPa) at SE-EPI MRE. The LS values from GRE and SE-EPI MRE were not significantly different (GRE 3.88 kPa vs. SE-EPI 4.14 kPa; $P = .19$). The median ROI area for measurement was significantly larger in SE-EPI than in GRE MRE (SE-EPI 7475.58 ± 3031.48 mm² vs. GRE 2571.39 ± 1885.91 mm², $P < .001$) (Figure 2).

While there was no technical failure in the SE-EPI group, 6 failures (12.5%) were

Table 3. Comparison of correlations between LS on each MRE sequence and TE in CHB versus non-CHB groups and LC versus non-LC groups

		CHB	Non-CHB	P	LC	Non-LC	P
Correlation coefficient (r)	SE-EPI MRE and TE	0.5018	0.9351	<.001	0.7795	0.9566	.003
	GRE MRE and TE	0.5830	0.8013	.16	0.6951	0.9585	.001

LS, liver stiffness; MRE, magnetic resonance elastography; TE, transient elastography; CHB, chronic hepatitis B; SE-EPI, spin-echo echo-planar imaging; GRE, gradient-recalled echo.
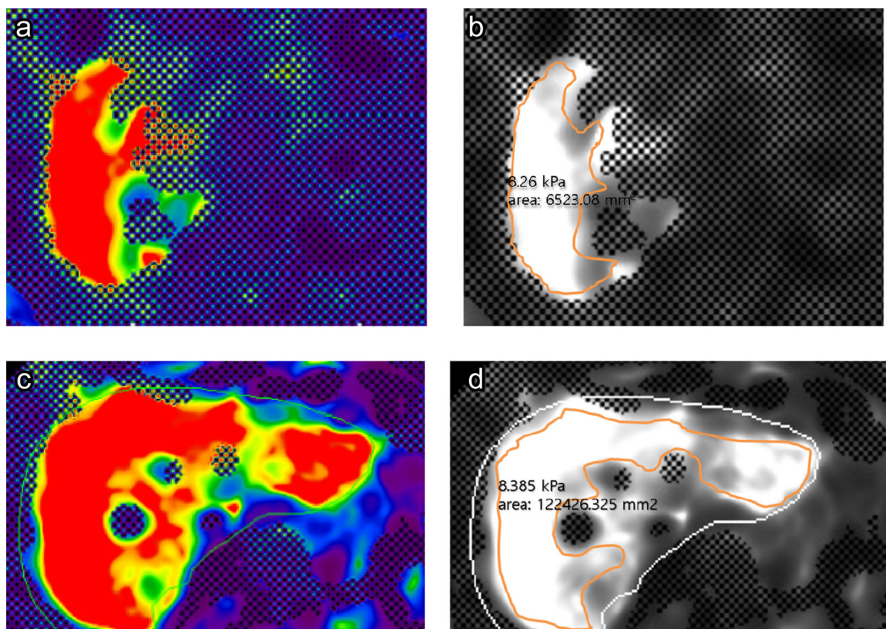
Figure 2. a-d. A 60-year-old man with multiple hepatocellular carcinomas in the liver. Representative GRE and SE-EPI MRE color elastogram **(a, c)** and gray-scale elastogram **(b, d)** images showed no significant difference between liver stiffness values measured from GRE MRE **(a, b)** and SE-EPI MRE **(c, d)**. The reliable area for measurement, without checkerboard pattern, is significantly larger with the elastogram **(c, d)** using SE-EPI sequence than those with the GRE sequence **(a, b)**, reflecting stability and reliability of the examination.
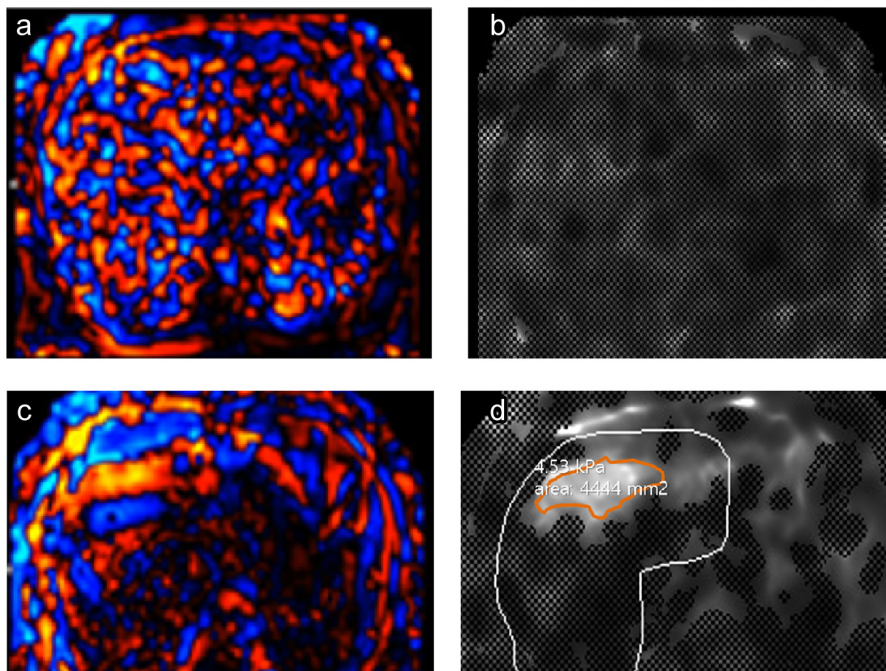
Figure 3. a-d. A 67-year-old man with alcoholic liver cirrhosis. Wave image **(a)** acquired during liver MRE examination using a 2-dimensional GRE sequence show irregular and bizarre pattern of the shear wave, likely indicating technical failure. However, wave image **(c)** acquired using a 2-dimensional SE-EPI sequence in the same patient show relatively regular and well-stratified shear wave indicating technical success. Furthermore, there is no pixel value with a confidence index higher than 95% in gray-scale elastogram **(b)** using GRE MRE when compared with elastogram **(d)** using SE-EPI MRE. The patient's automatically calculated R2* (1/T2*) value from a 3-dimensional multi-echo Dixon sequence (LiverLab, Siemens Healthcare) was 187.5/s which indicates iron deposition and also is known to result in a higher technical failure rate in GRE MRE.

found in the GRE MRE group. All patients with failure in the GRE MRE group had LC

in morphological analyses. Among them, 1 patient had significant iron deposition

(Figure 3) and another had BMI greater than 30; that is 30.1. The technical success rates in both MRE scans were significantly different (100.0% (SE-EPI) vs. 87.5% (GRE), $P = .03$). Meanwhile, none of the parameters were found to be significantly associated with GRE MRE failure in the univariate analysis (all $P > .05$). The characteristics of the failure group are summarized in Table 4.

Discussion

Our study demonstrated that the LS results between TE and MRE generated by SE-EPI and GRE sequences strongly correlated with each other ($r = 0.79$, $P < .001$ and $r = 0.74$, $P < .001$, respectively). To our knowledge, there has been no study to compare the hepatic stiffness obtained by GRE MRE, SE-EPI MRE, and TE in the same study population. In previous studies comparing GRE MRE and TE,[16,24,25,30] GRE MRE correlated well with TE and had better diagnostic performance than TE for detection and staging of hepatic fibrosis. Nevertheless, few studies have evaluated the correlation between SE-EPI MRE and TE. The only prior study published in English[26] showed comparable accuracy for diagnosing significant fibrosis in TE and SE-EPI MRE in patients with CHB and CHC. Moreover, our results showed a good correlation among non-invasive techniques for hepatic fibrosis, that is SE-EPI MRE, GRE MRE, and TE.

Regarding etiology of hepatic fibrosis, we observed a less correlation between LS values from SE-EPI and TE in the CHB group, as compared to the non-CHB group in our study. Previous literature has shown a lower sensitivity of TE or MRE in patients with CHB than in those without CHB.[31-34] Our results might be due to the fact that histopathologic presentation of hepatitis B differs from other etiologies such as hepatitis C.[31] Histologic features of CHB patients are known to have a tendency to become macronodular and heterogeneous in the liver and thus, result in LS values that vary depending on the region of the liver and necro-inflammatory activity.[31,32,35]

Correlations between LS values measured on MRE and TE were significantly stronger in patients without LC patients than in patients with LC in both MR sequences. This may be attributed to the heterogeneous distribution of hepatic

Table 4. Characteristics of the failure group

Failure on GRE MRE	Presence of LC	CTP score	R2*(s⁻¹)	BMI (kg/m²)	Ascites	Etiology of CLD
Patient 1	Yes	A	70.1	23.6	None	HBV
Patient 2	Yes	B	48	22.5	Scanty	HBV
Patient 3	Yes	A	187.5	29.7	Scanty	Alcohol abuse
Patient 4	Yes	A	43.2	30.1	Scanty	Autoimmune
Patient 5	Yes	B	57.2	23.5	Scanty	HBV
Patient 6	Yes	A	58.4	23.7	None	N/A

GRE, gradient-recalled echo; MRE, magnetic resonance elastography; LC, liver cirrhosis; CTP, Child–Turcotte–Pugh; BMI, body mass index; CLD, chronic liver disease; HBV, hepatitis B virus; N/A, non-applicable.

fibrosis, which results in the risk of sampling error.[36,37] While larger sample volumes can be evaluated by MRE, TE measures tissue stiffness over a 1 × 4 cm region of tissue,[29] making the evaluation of cirrhotic liver tissue less reliable.

Our study showed a significantly higher technical success rate of SE-EPI MRE than that of GRE MRE without a significant difference in LS values. This result may be related to the significantly larger ROI-measurable area in the confidence maps of SE-EPI MRE than those of GRE MRE. Furthermore, the SE-EPI MRE would enable a more generalized assessment of the liver elasticity (Figure 2). These results are consistent with those of several prior studies,[20,23,38,39] in which SE-EPI MRE resulted a higher technical success rate, larger measurable ROI area, and improved subjective image quality compared to GRE MRE.

One of the 2 patients, whose LS value did not fall within the 95% prediction limits of agreement for GRE MRE versus TE, had large ascites which is known to lead to less reliable results in both TE and MRE.[13,38] The other patient had previously undergone chemoembolization for ruptured HCC in the right hemi-liver. In MRE, ROIs could be drawn excluding the mass, but the LS measurement may have included the lipiodolized portion of the mass, resulting in the overestimation of hepatic stiffness. Meanwhile, as it is known that technical failure rates in GRE MRE increase as the deposition of iron in the liver increases,[20] LS evaluation failed in the patient (n = 1) with significant hepatic iron deposition in our study (Figure 3).

Despite intense interest in alternative approaches to evaluating hepatic fibrosis, there is no consensus on the optimal approach for liver fibrosis assessment. TE is highly portable, widely available, and may be preferred over MRE in routine screening

of advanced fibrosis in a low-risk patient due to its cost-effectiveness. On the other hand, the MRI-based approach may be preferable when more comprehensive liver imaging examination is needed or when the patient is unable (e.g., obesity or ascites) to undergo TE. The clinical importance of our study is that SE-EPI and GRE MRE sequences can be alternatives for TE and vice versa.

This study has several limitations. First, it constitutes a relatively small study population of only 48 patients. This also limits the evaluation of the performance of MRE and TE according to the degree of BMI, iron deposition, amount of ascites, or each etiologic cause. Second, the obtained LS values with both MRE and TE were not compared to histologic fibrosis through biopsy, which traditionally is considered to be the reference standard for staging fibrosis, due to its invasiveness and significant cost. Third, slice thickness and gaps for GRE-MRE were 5/10 mm while those for SE-MRE were 6/12 mm, which means exact slice levels are different for these 2 MREs. Fourth, all patients underwent MRE examinations using a single MR unit in this single-institution study. Therefore, a future prospective study in a large patient population using multiple MR units will be necessary.

In conclusion, we found a strong association of LS values measured by TE with those of GRE and SE-EPI MRE techniques, respectively, especially in non-CHB and non-LC patients. We also found GRE and SE-EPI MRE stiffness measurements to be strongly correlated even though SE-EPI-MRE resulted a significantly higher technical success rate than GRE-MRE. Therefore, we believe that TE, GRE, and SE-EPI MRE techniques may complement each other according to the appropriate individual situation.

References

1. Iredale JP. Models of liver fibrosis: exploring the dynamic nature of inflammation and repair in a solid organ. *J Clin Invest*. 2007;117(3):539-548. [CrossRef]
2. Dixon JB, Bhathal PS, Hughes NR, O'Brien PE. Nonalcoholic fatty liver disease: improvement in liver histological analysis with weight loss. *Hepatology*. 2004;39(6):1647-1654. [CrossRef]
3. Calvaruso V, Craxi A. Regression of fibrosis after HBV antiviral therapy. Is cirrhosis reversible? *Liver Int*. 2014;34(suppl 1):85-90. [CrossRef]
4. Venkatesh SK, Ehman RL. Magnetic resonance elastography of liver. *Magn Reson Imaging Clin N Am*. 2014;22(3):433-446. [CrossRef]
5. Chen J, Yin M, Glaser KJ, Talwalkar JA, Ehman RL. MR elastography of liver disease: state of the art. *Appl Radiol*. 2013;42(4):5-12.
6. Frulio N, Trillaud H. Ultrasound elastography in liver. *Diagn Interv Imaging*. 2013;94(5):515-534. [CrossRef]
7. Afdhal NH, Nunes D. Evaluation of liver fibrosis: a concise review. *Am J Gastroenterol*. 2004;99(6):1160-1174. [CrossRef]
8. Sandrin L, Fourquet B, Hasquenoph JM, et al. Transient elastography: a new noninvasive method for assessment of hepatic fibrosis. *Ultrasound Med Biol*. 2003;29(12):1705-1713. [CrossRef]
9. Fraquelli M, Rigamonti C, Casazza G, et al. Reproducibility of transient elastography in the evaluation of liver fibrosis in patients with chronic liver disease. *Gut*. 2007;56(7):968-973. [CrossRef]
10. Kennedy P, Wagner M, Castéra L, et al. Quantitative elastography methods in liver disease: current evidence and future directions. *Radiology*. 2018;286(3):738-763. [CrossRef]
11. Neukam K, Recio E, Camacho A, et al. Interobserver concordance in the assessment of liver fibrosis in HIV/HCV-coinfected patients using transient elastometry. *Eur J Gastroenterol Hepatol*. 2010;22(7):801-807. [CrossRef]
12. Castéra L, Foucher J, Bernard PH, et al. Pitfalls of liver stiffness measurement: a 5-year prospective study of 13,369 examinations. *Hepatology*. 2010;51(3):828-835. [CrossRef]
13. Foucher J, Castéra L, Bernard PH, et al. Prevalence and factors associated with failure of liver stiffness measurement using FibroScan in a prospective study of 2114 examinations. *Eur J Gastroenterol Hepatol*. 2006;18(4):411-412. [CrossRef]

14. Bonekamp S, Kamel I, Solga S, Clark J. Can imaging modalities diagnose and stage hepatic fibrosis and cirrhosis accurately? *J Hepatol*. 2009;50(1):17-35. [CrossRef]

15. Yin M, Glaser KJ, Talwalkar JA, Chen J, Manduca A, Ehman RL. Hepatic MR elastography: clinical performance in a series of 1377 consecutive examinations. *Radiology*. 2016;278(1):114-124. [CrossRef]

16. Dyvorne HA, Jajamovich GH, Bane O, et al. Prospective comparison of magnetic resonance imaging to transient elastography and serum markers for liver fibrosis detection. *Liver Int*. 2016;36(5):659-666. [CrossRef]

17. Venkatesh SK, Yin M, Ehman RL. Magnetic resonance elastography of liver: technique, analysis, and clinical applications. *J Magn Reson Imaging*. 2013;37(3):544-555. [CrossRef]

18. Huwart L, Sempoux C, Vicaut E, et al. Magnetic resonance elastography for the noninvasive staging of liver fibrosis. *Gastroenterology*. 2008;135(1):32-40. [CrossRef]

19. Kim YS, Jang YN, Song JS. Comparison of gradient-recalled echo and spin-echo echo-planar imaging MR elastography in staging liver fibrosis: a meta-analysis. *Eur Radiol*. 2018;28(4):1709-1718. [CrossRef]

20. Wagner M, Besa C, Ayache JB, et al. MR elastography of the liver: qualitative and quantitative comparison of gradient echo and spin echo echoplanar imaging sequences. *Invest Radiol*. 2016;51:575-581.

21. Huwart L, Salameh N, Ter Beek L, et al. MR elastography of liver fibrosis: preliminary results comparing spin-echo and echo-planar imaging. *Eur Radiol*. 2008;18(11):2535-2541. [CrossRef]

22. Garteiser P, Sahebjavaher RS, Ter Beek LC, et al. Rapid acquisition of multifrequency, multislice and multidirectional MR elastography data with a fractionally encoded gradient echo sequence. *NMR Biomed*. 2013;26(10):1326-1335. [CrossRef]

23. Choi SL, Lee ES, Ko A, et al. Technical success rates and reliability of spin-echo echo-planar imaging (SE-EPI) MR elastography in patients with chronic liver disease or liver cirrhosis. *Eur Radiol*. 2019:1-8.

24. Ichikawa S, Motosugi U, Morisaka H, et al. Comparison of the diagnostic accuracies of magnetic resonance elastography and transient elastography for hepatic fibrosis. *Magn Reson Imaging*. 2015;33(1):26-30. [CrossRef]

25. Hsu C, Caussy C, Imajo K, et al. Magnetic resonance vs transient elastography analysis of patients with nonalcoholic fatty liver disease: a systematic review and pooled analysis of individual participants. *Clin Gastroenterol Hepatol*. 2019;17(4):630-637.e8. [CrossRef]

26. Bohte AE, de Niet A, Jansen L, et al. Non-invasive evaluation of liver fibrosis: a comparison of ultrasound-based transient elastography and MR elastography in patients with viral hepatitis B and C. *Eur Radiol*. 2014;24(3):638-648. [CrossRef]

27. Kannengiesser S. Iron quantification with LiverLab. *MAGNETOM Flash*. 2016;66:44-46.

28. d'Assignies G, Paisant A, Bardou-Jacquet E, et al. Non-invasive measurement of liver iron concentration using 3-tesla magnetic resonance imaging: validation against biopsy. *Eur Radiol*. 2018;28(5):2022-2030. [CrossRef]

29. Ferraioli G, Filice C, Castera L, et al. WFUMB guidelines and recommendations for clinical use of ultrasound elastography: part 3: liver. *Ultrasound Med Biol*. 2015;41(5):1161-1179. [CrossRef]

30. Oudry J, Chen J, Glaser KJ, Miette V, Sandrin L, Ehman RL. Cross-validation of magnetic resonance elastography and ultrasound-based transient elastography: a preliminary phantom study. *J Magn Reson Imaging*. 2009;30(5):1145-1150. [CrossRef]

31. Castera L, Forns X, Alberti A. Non-invasive evaluation of liver fibrosis using transient elastography. *J Hepatol*. 2008;48(5):835-847. [CrossRef]

32. Kim SU, Han KH, Ahn SH. Transient elastography in chronic hepatitis B: an Asian perspective. *World J Gastroenterol*. 2010;16(41):5173-5180. [CrossRef]

33. Udompap P, Sukonrut K, Suvannarerg V, Pongpaibul A, Charatcharoenwitthaya P. Prospective comparison of transient elastography, point shear wave elastography, Apri and FIB-4 for staging liver fibrosis in chronic viral hepatitis. *J Viral Hepat*. 2020;27(4):437-448. [CrossRef]

34. Chang W, Lee JM, Yoon JH, et al. Liver fibrosis staging with MR elastography: comparison of diagnostic performance between patients with chronic hepatitis B and those with other etiologic causes. *Radiology*. 2016;280(1):88-97. [CrossRef]

35. Sporea I, Şirli R, Deleanu A, et al. Liver stiffness measurements in patients with HBV vs HCV chronic hepatitis: a comparative study. *World J Gastroenterol*. 2010;16(38):4832-4837. [CrossRef]

36. Bedossa P, Dargère D, Paradis V. Sampling variability of liver fibrosis in chronic hepatitis C. *Hepatology*. 2003;38(6):1449-1457. [CrossRef]

37. Rousselet MC, Michalak S, Dupré F, et al. Sources of variability in histological scoring of chronic viral hepatitis. *Hepatology*. 2005;41(2):257-264. [CrossRef]

38. Wagner M, Corcuera-Solano I, Lo G, et al. Technical failure of MR elastography examinations of the liver: experience from a large single-center study. *Radiology*. 2017;284(2):401-412. [CrossRef]

39. Kim YS, Song JS, Kannengiesser S, Seo SY. Comparison of spin-echo echoplanar imaging and gradient recalled echo-based MR elastography at 3 tesla with and without gadoxetic acid administration. *Eur Radiol*. 2017;27(10):4120-4128. [CrossRef]